RSC Advances

PAPER

View Article Online
View Journal | View Issue

Cite this: *RSC Adv.*, 2026, **16**, 21756

Differentiation of β-phosphorylated nitroxide diastereoisomers by complexation with cyclodextrins: an EPR and cyclic voltammetry study

Alexandru Gabriel Bucur,[a] Nicolae Spataru,[a] Sylvain R. A. Marque, *[ab] Loredana Preda,[a] Jean-Patrick Joly,[ab] Gerard Audran,[b] Mathilde Trapp,[b] Tanta Spataru,[a] Florenta Savonea[a] and Gabriela Ionita *[a]

The complexation of two diastereoisomers of a β-phosphorylated cyclic nitroxide radical (2,5-dimethyl-5-hydroxymethylene-2-diethoxyphosphonyl-pyrrolidin-*N*-oxyl) with cyclodextrins (β-CD and γ-CD) was investigated using electron paramagnetic resonance (EPR) spectroscopy and cyclic voltammetry. The two isomers have different EPR signatures due to the differences in their phosphorus and nitrogen hyperfine splitting constants. The *cis* stereoisomer (1c$^{\bullet}$) promotes intramolecular hydrogen bonding, involving the HO group attached to the methylene group and O atom from the phosphorus moiety, while in the case of the *trans* stereoisomer (1t$^{\bullet}$), this intramolecular bonding is not possible. The EPR spectra indicate the higher affinity of the 1t$^{\bullet}$ isomer for γ-CD, highlighting the different EPR parameters of the free radical and complexed radical. The binding constants determined based on the EPR and cyclic voltammetry data show stronger affinity for γ-CD compared with β-CD, particularly for 1t$^{\bullet}$. An increasing potassium chloride concentration enhances the stability of the complex linearly by modulating the solvation and electrostatic interactions, as indicated by the thermodynamic parameters obtained from EPR measurements. Electrochemical measurements demonstrate decreased diffusion coefficients and anodic peak shifts upon complexation, supporting the spectroscopic results. These findings highlight the important role of molecular stereochemistry and ionic strength in modulating host–guest interactions between cyclodextrins and nitroxides.

Received 30th January 2026
Accepted 7th April 2026

DOI: 10.1039/d6ra00820h

rsc.li/rsc-advances

Introduction

Host–guest chemistry of stable radicals has been investigated for decades using electron paramagnetic resonance (EPR) spectroscopy. Most studies have focused on the complexation of nitroxides with cyclodextrins (CDs),[1,2] while a limited number of studies have investigated other types of radicals, including β-phosphorylated nitroxides.

In contrast to nitroxides, for which host–guest interactions induce a modest decrease in the N-atom hyperfine splitting constant of up to 1 G, in the case of β-phosphorylated nitroxides, the changes in the hyperfine splitting constants of N-atom and P-atom are more substantial, as they can be influenced both by the more hydrophobic microenvironment of the cavity and by changes in the geometry of the radical as a result of inclusion in the cavity.

We previously investigated the host–guest complexes of four β-phosphorylated nitroxides having cyclic and non-cyclic structures with CDs, highlighting the conformational changes induced by complexation in the case of an acyclic nitroxide.[3,4] Interestingly, it was found that the EPR parameters of one of the acyclic compounds are dependent on the cavity size of the host molecules, making it possible to differentiate their presence in a mixture of CDs. In this way, it was demonstrated that β-phosphorylated nitroxides are more suitable spin probes to investigate host–guest complexes as they provide more detailed information compared with the classical nitroxides.[3] However, the role of diastereoisomerism in the complexation of β-phosphorylated cyclic nitroxides with CDs and the influence of ionic strength on this process have not been examined in detail. Therefore, in the present work, we investigated the inclusion complexes formed by the geometrical isomers of a β-phosphorylated nitroxide (Fig. 1) with β- and γ-CDs using EPR spectroscopy and cyclic voltammetry, with particular attention to the effects of stereochemistry, host cavity size, and ionic strength. Analysis of the EPR parameters of stable radicals in water and CD solutions can lead to the evaluation of host–guest

[a]"Ilie Murgulescu" Institute of Physical Chemistry of the Romanian Academy, 202 Splaiul Independentei, Bucharest 060021, Romania. E-mail: ige@icf.ro; gabi2ionita@yahoo.com; abucur@icf.ro; nspataru@icf.ro; sylvain.marque@univ-amu.fr; predalore@yahoo.com; jean-patrick.joly@univ-amu.fr; tspataru@icf.ro; fsavonea@icf.ro

[b]Aix Marseille Univ., CNRS, ICR, UMR 7273, Case 551, Avenue Escadrille Normandie-Niemen, 13397, Marseille Cedex 20, France. E-mail: g.audran@univ-amu.fr; mathilde.trapp@univ-amu.fr

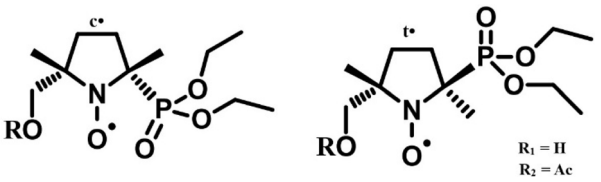

Fig. 1 Structures of the *cis* (1c• and 2c•) and *trans* (1t• and 2t•) isomers used in this study.

association constants, which has been already extensively studied for various systems.[1–6] In turn, cyclic voltammetry is used sporadically for studying host–guest complexes.[7–13] Combining these two physicochemical methods provides information on the binding process, highlighting the factors that may influence the process. The presence of a hydroxyl group in the structure of these radicals influences their structural features and hence their EPR parameters, but at the same time they are precursors for obtaining new functionalized spin probes that can find application in bioimaging.

Materials and methods

The β-phosphorylated nitroxides 1c• and 1t• were prepared as previously reported.[14] β-CD and γ-CD were purchased from Alfa Aesar and KCl from Fluka and were used as received.

The EPR spectra were recorded on an X-band JEOL FA100 EPR spectrometer equipped with a TE011 cylindrical-type resonator using the following settings: frequency modulation of 100 kHz, microwave power of 0.998 mW, modulation amplitude of 0.5 G, sweep width of 150 G, sweep time of 240 s, and time constant of 0.1 s.

Stock solutions of the spin probes (10^{-2} M) were prepared in ethanol and appropriate volumes of these solutions were evaporated and the spin probes were redissolved in water to reach a concentration of 2.5×10^{-4} M, in the absence or in the presence of CDs (in the range of 10^{-5} to 10^{-2} M for β-CD and 10^{-5} to 5×10^{-2} M for γ-CD).

EPR spectra were simulated with the WinSim software available from NIEHS[15] using the LMB1 optimization algorithm, and with the EasySpin software[16] using the garlic core function for isotropic and fast-motion continuous wave EPR spectra.

Cyclic voltammetry experiments were performed in a 0.5 M KCl aqueous solution at room temperature, using a PAR 273 A potentiostat in a three-electrode glass cell. A glassy carbon (3 mm diameter) from Ossila was used as the working electrode, which was polished with an aqueous alumina slurry and thoroughly rinsed with double-distilled water before each experiment. A platinum wire and Ag/AgCl electrode were used as the counter and reference electrodes, respectively.

The geometries of β-phosphorylated nitroxides 1c• and 1t• were investigated by density functional theory (DFT) using the B3LYP functional and the 6-311++G(d,p) basis set as implemented in Gaussian 09.[17] Initial structures were generated from the available X-ray diffraction geometry, and several starting conformations were considered to account for the rotational flexibility of the hydroxymethyl and phosphonate substituents. Geometry optimizations were followed by frequency calculations to confirm that the obtained structures correspond to true minima on the potential energy surface. To account for solvent effects relevant to the experimental conditions, additional calculations were performed in water using the SMD implicit solvation model.

Results and discussion

The EPR parameters of stable radicals are sensitive to their inclusion in cyclodextrins. Thus, the rotational correlation time for a nitroxide increases as a result of the inclusion of the radical in the cyclodextrin cavity, and usually the association constant can be calculated from its variation with the cyclodextrin concentration.[18,19] The second parameter is the hyperfine splitting constant a_N, which provides information on the polarity of the microenvironment surrounding the paramagnetic group (Fig. 2a). Analysis of this parameter usually provides information on how inclusion in the cyclodextrin cavity occurs. In the case of β-phosphorylated nitroxide radicals, their EPR parameters are defined by the mesomeric forms of the two groups that determine the interaction of a free electron with the N and P nuclei and the dihedral angle θ between the singly occupied molecular orbital (SOMO) of the N atom and the σC–P bond (Fig. 2).[20]

Although in the case of classical nitroxides, a direct correlation can be established between the polarity of the medium and the hyperfine splitting constant, for β-phosphorylated nitroxides, the variations in the hyperfine splitting constant a_P do not reflect only the polarity of the medium. This situation is determined by changes in the angle θ, in other words, by geometrical changes in the radical, depending on the nature of the solvent. The presence of hydroxyl groups in the structures of the two diastereoisomers considered in the current study favours the formation of intramolecular hydrogen bonds (IHBs). Depending on the polarity of the solvent, and also on interactions with other molecular species (such as the cyclodextrin host molecules in this study), conformational changes may occur.

DFT calculations indicate that the hydroxyl group is involved in an IHB only for the 1c• isomer. In the case of 1t•, the O···H distance of 3.11 Å is larger than the sum of the van der Waals radii, and also the 109° angle between the OH group and the oxygen atom of the nitroxide group is small for an IHB, while in the *cis* 1c• isomer, the OH group interacts with the diethyl

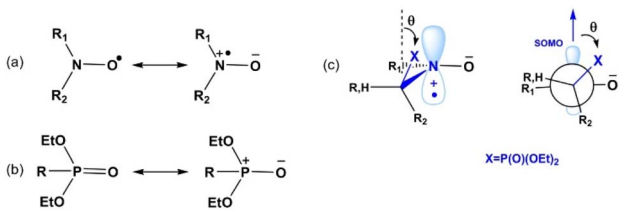

Fig. 2 Mesomeric forms of the nitroxyl (a) and phosphoryl (b) moieties. Dihedral angle θ between the SOMO and the C–P bond (c).

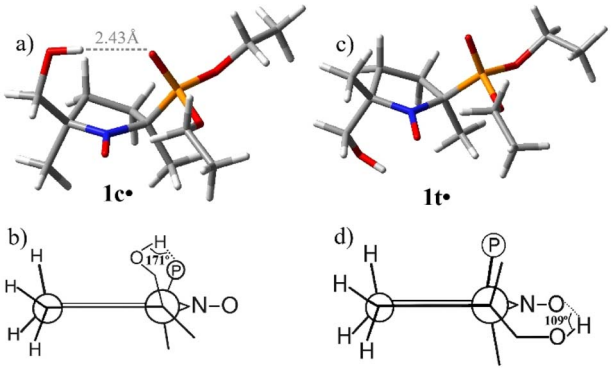

Fig. 3 Geometries of 1c• (a and b) and 1t• (c and d) obtained with the optimization and frequency calculations performed at the DFT level with Gaussian 09.

phosphoryl group, resulting in a shorter O···H distance of 1.85 Å. This theoretical description of IHB formation provides a basis for predicting the behaviour of these probes in solution. In particular, it is predicted that the breaking of the OH···O=P hydrogen bond in 1c• will directly influence the hyperfine coupling constant of the P atom and may induce conformational changes that can be monitored by the variations in θ (Fig. 3).

For 1c•, its OH···O=P distance is shorter than the sum of the van der Waals radii (2.72 Å), and its ⟨O–H···OP⟩ value of 171° is consistent with the presence of a strong IHB between the hydroxy and phosphoryl groups, while the longer OH···ON distance and smaller angle indicate the likely absence of significant IHB between OH and the nitroxide oxygen. In contrast, for 1t•, where the OH and $P(O)(OEt)_2$ groups adopt a *trans* arrangement, the large $d_{OH\cdots OP}$ and the closed ⟨O–H···OP⟩ angle exclude any meaningful IHB involving the phosphoryl oxygen.[21] The calculated geometrical parameters are in reasonable agreement with the X-ray diffraction data[14] with respect to the key bond lengths and the overall relative orientation of the nitroxide, hydroxymethyl, and phosphonate fragments, while differences are expected because the crystallographic structure corresponds to the solid state, whereas the present calculations are for solvated molecules (Table 1).

Table 1 Geometrical parameters obtained from the DFT (1c• and 1t•) and XRD (1t•) analyses[a]

	1c• DFT	1t• DFT	1t• XRD[14]
OH–ON	3.26 Å	3.11 Å	3.27 Å
O–H–ON	103°	109°	102°
OH–OP	2.43 Å	5.89 Å	5.82 Å
O–H–OP	171°	96.9°	76°
N–O	1.28 Å	1.28 Å	1.27 Å
C–P	1.87 Å	1.87 Å	1.83 Å
O–N–C–P	−54.4°	−60.7°	−73.7°
O–N–C–COH	−52.6°	−59.5°	−63.7°

[a] van der Waals radii for: H = 1.20 Å, O = 1.52 Å, N = 1.55 Å, and P = 1.80 Å.[21]

Table 2 Hyperfine splitting constant values for the free (water) and complexed isomers in β-CD (10^{-2} M) and γ-CD (5×10^{-2} M)

	1c•		1t•	
	a_N [G]	a_P [G]	a_N [G]	a_P [G]
Pentane[23]	13.12	43.19	13.86	48.02
Water	15.06	44.92	14.77	47.75
β-CD	14.56	44.31	14.11	48.33
γ-CD	14.38	46.42	14.09	52.42
Water (0.5 M KCl)	15.08	44.94	14.78	47.72
β-CD (0.5 M KCl)	14.59	44.34	14.13	48.31
γ-CD (0.5 M KCl)	14.41	46.38	14.11	52.39

The EPR spectroscopic investigation of the sterically constrained β-phosphorylated nitroxides isomers 1c• and 1t• reveals significant differences in their EPR parameters. Analysis of the experimental spectra of the two isomers reveals that 1t• has a higher a_P than isomer 1c• (Table 2). The polarity of the surrounding microenvironment of the radical influences the values of a_N. For isomers 1c• and 1t•, in pentane and in the presence of cyclodextrins, a_N decreases, indicating a less hydrophilic environment than water.[22]

The decrease in the a_N value in the presence of cyclodextrins for the two isomers is similar, proving the inclusion of the nitroxyl group in the cavities of the host molecules. The variation in the a_N value is less than 1 G, which is also observed for simple nitroxides.[5,6] Upon complexation, the most significant changes are observed in the EPR spectrum of 1t• in γ-CD (at the highest concentration of 5×10^{-2} M), which presents a two-component pattern (Fig. 4), indicating that the complexed species and the free species have clearly different parameters. Simulation of the EPR spectra of the two isomers provided the EPR parameters corresponding to each concentration of cyclodextrins (SI, Tables S1 and S2).

For the phosphorus hyperfine splitting constant a_P, a consistent difference of approximately 3 G between the two isomers is observed in aqueous solution, which can be attributed to the distinct spatial orientation of the phosphorus atom relative to the unpaired electron.

Upon complexation with cyclodextrins, this difference in a_P is further amplified. Specifically, an increase of 4 G is observed upon inclusion in β-CD and 6 G increase in the case of γ-CD. This enhancement is associated with changes in the dihedral

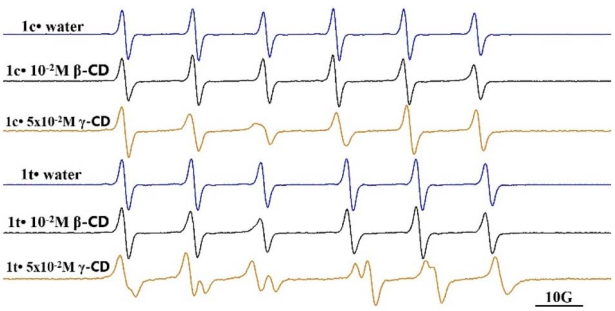

Fig. 4 EPR spectra of the 1c• and 1t• radicals in water and in the highest concentration of CD solutions.

angle induced by the inclusion of the radical into the cyclodextrin cavity, which perturbs the local conformation of the molecule.

The different complexation abilities of the two cyclodextrins are further reflected in the hyperfine coupling constants of the P-atom. It can be observed that, with the exception of 1c$^{\bullet}$ in pentane and β-CD, in all cases, the a_P values increase in nonpolar media.

The intramolecular H bond that forms between the hydroxyl group and the phosphoryl group in this isomer limits the rotation of the phosphoryl group. In the case of γ-CD, the complexation is stronger and, due to the larger dimensions of the cavity of this cyclodextrin, deeper inclusion is ensured compared to β-CD. The inclusion process leads to a new conformation that disrupts the IHB, and a_P follows the same trend as the other systems. For 1c$^{\bullet}$, a_P differs by approximately 2 G between the β-CD and γ-CD complexes, while for 1t$^{\bullet}$, the difference is more pronounced at around 4 G. This greater variation for the 1t$^{\bullet}$ complex is a consequence of its *trans* configuration, which does not allow IHBs in aqueous solution between the hydroxyl group and the phosphoryl oxygen (O=P). Thus, the geometry is more easily disturbed upon inclusion in the cyclodextrin cavity, leading to conformational rearrangement and a greater change in the dihedral angle θ. These results are correlated with the previously reported radicals 2c$^{\bullet}$ and 2t$^{\bullet}$. For both, their a_P values increase in pentane compared with water.[14]

The a_P values are determined by the value of the angle θ according to the Heller–McConnell relationship (eqn (1)),[24] as follows:

$$a_{P,\beta} = B_0 + B_1 \times \rho_N^{\pi} \cos^2 \theta, \quad (1)$$

where B_0 is the constant for the transfer of spin density through the spin polarization process (in general disregarded), B_1 is the constant for the transfer of spin density through the hyperconjugation process, ρ_N^{π} is the spin density on the nitrogen atom, and θ the dihedral angle between the SOMO and the σC–P bond.

As a_N is proportional to ρ_N^{π}, we can use eqn (2) to estimate the conformational changes reflected by the ratio of the $\cos^2 \theta$ values in two environments, as follows:

$$\frac{a_{P,1}}{a_{P,n}} = \frac{a_{N,1}}{a_{N,n}} \times \frac{\cos^2 \theta_1}{\cos^2 \theta_n}, \quad (2)$$

where $a_{P,1}$ and $a_{N,1}$ refer to the parameters for the free radical in the bulk solvent, while $a_{P,n}$ and $a_{N,n}$ refer to the parameters of the radical in a cyclodextrin complex, respectively.

Starting from the value of the $(\cos^2 \theta_1)/(\cos^2 \theta_n)$ ratio, it is possible to evaluate the decrease in θ as a consequence of complexation. The values of θ for radicals 1c$^{\bullet}$ and 1t$^{\bullet}$ corresponding to their complexes with β-CD and γ-CD relative to the values of a_N and a_P in water are shown in Table 3. This table also presents the values of θ corresponding to pentane to highlight the influence of the inclusion process. The variation of θ, denoted by $\Delta\theta$, is expressed relative to the value in water. The most substantial shift in θ is observed for 1t$^{\bullet}$ upon complexation with γ-CD, where $\cos^2 \theta_2$ increases by approximately 15% compared to the free radical. This strongly supports the hypothesis that the inclusion process disrupts the radical conformation more easily when the IHB with the phosphoryl group is absent.

Table 3 Changes in θ values and the corresponding $\cos^2 \theta$ values determined by complexation with cyclodextrins

	1c$^{\bullet}$			1t$^{\bullet}$			2c$^{\bullet}$	2t$^{\bullet}$
	θ (°)	$\Delta\theta$ (°)	$\cos^2 \theta_2$	θ (°)	$\Delta\theta$ (°)	$\cos^2 \theta_2$	θ (°)	θ (°)
Water	36.2°	—	—	29.7°	—	—	36	32
β-CD	35.4°	0.8°	+2%	26.7°	3.0°	+6%	—	—
γ-CD	32.9°	3.3°	+8%	21.4°	8.3°	+15%	—	—
Pentane	32.0°	4.2°	+11%	26.0°	3.7°	+7%	27	19

These spectroscopic findings are corroborated by the association constants, which demonstrate stronger binding affinities for γ-CD compared to β-CD. Specifically, the association constants (K, M^{-1}) for 1c$^{\bullet}$ are 44.3 M^{-1} and 72.6 M^{-1} with β-CD and γ-CD, whereas for 1t$^{\bullet}$, these values increase to 48.7 M^{-1} and 142.3 M^{-1}, respectively, indicating a more pronounced enhancement in complexation in the 1t$^{\bullet}$/CD systems. The stronger binding of the *trans* isomer is related to its molecular geometry. In particular, the *trans* arrangement provides a more favourable spatial disposition of the substituents relative to the pyrrolidine ring, which may reduce steric hindrance during its inclusion and allow a more efficient host–guest fit, especially in the larger γ-CD cavity.

The association constants were evaluated using eqn (3), as follows:

$$K = \frac{[\text{complexed species}]}{[\text{free species}] \times [\text{free cyclodextrin}]}. \quad (3)$$

The association constants were calculated using the proportion of the spin probe in the bulk solvent (free) and in the complexed form for each concentration of cyclodextrin obtained by simulation of EPR spectra. For each spin probe/cyclodextrin pair, the association constant value was taken as the average of the values determined at each cyclodextrin concentration. Furthermore, insights into the dynamic behaviour of the radicals were gained through the calculation of the rotational correlation time, τ. A one-order-of-magnitude increase in τ was observed upon complexation, indicating reduced molecular mobility due the increased effective size of

Table 4 Correlational rotational time values for 1c$^{\bullet}$ and 1t$^{\bullet}$ in water and cyclodextrin solutions

	$\tau \times 10^{10}$ s		
Sample	Water (free)	β-CD (complexed)	γ-CD (complexed)
1c$^{\bullet}$	2.5	16.6	17.4
1t$^{\bullet}$	2.4	20.3	21.9

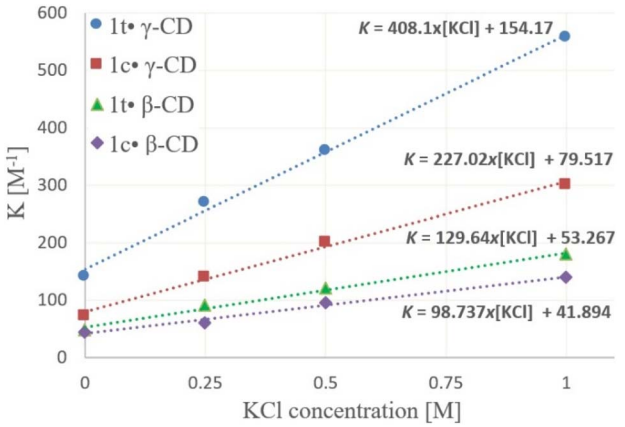

Fig. 5 Graphical representation of the association constant value as a function of the KCl concentration.

the complex.[25] The complexes with γ-CD exhibit slightly higher τ values compared to those with β-CD, consistent with its larger size and deeper inclusion geometry. Between the two isomers, the 1c• complexes demonstrate slightly lower τ values, potentially attributed to their more compact complex geometry, which allows for slightly enhanced rotational freedom (Table 4).

Since cyclic voltammetry measurements require the presence of an electrolyte, its effect on the EPR parameters of the two diastereoisomers was investigated, both in the absence and in the presence of cyclodextrins. Thus, the inclusion complexation between the radicals and cyclodextrins was investigated under varying concentrations of potassium chloride (KCl) to assess the influence of ionic strength on complex stability.

This investigation may provide insights into how ionic strength can influence the process of radical inclusion in cyclodextrins, with the results being relevant for correlating the data obtained from electrochemical measurements. A series of measurements was performed to determine the inclusion constants (K) of the two radicals with β-CD and γ-CD at different KCl concentrations. Linear regression analysis of the data (Fig. 5) revealed a direct correlation between the inclusion constant and the electrolyte concentration, as described by eqn (4) as follows:

$$K = S[\mathrm{KCl}] + K_0. \quad (4)$$

The slope represents the sensitivity of the inclusion process to ionic strength, while the intercept corresponds to the intrinsic stability of the complex in the absence of added salt.

This slope quantifies the empirical sensitivity of inclusion to ionic strength and represents how much K increases for each mole of salt added, $S = \mathrm{d}K/(\mathrm{d}[\mathrm{KCl}])$. The values of S found for each complex are presented in Table 5.

The a_N and a_P values of the two radicals were not influenced by the presence of salt in the solutions. This suggests that the electrolyte concentration, and therefore ionic strength, exerts a significant effect on the stability of the host–guest complex formed. The enhancement in complex stability with an increase in the electrolyte concentration can be attributed to the disruption of the solvation dynamics and electrostatic interactions in the system. Nitroxides, possessing polar N–O• groups, are solvated in aqueous media due to dipole–dipole interactions and hydrogen bonding with surrounding water molecules.

This hydration shell stabilizes the radical in bulk solution and opposes its transfer into the relatively hydrophobic cavity of cyclodextrins. The ease with which the radical forms a complex in the absence of potassium chloride influences the extent to which its complexing ability is enhanced upon the addition of KCl. Specifically, radicals with a higher affinity for complexation show a proportionally greater increase in binding capacity in the presence of potassium chloride compared to radicals with lower basic affinities.

This relationship is quantitatively reflected in the slopes of the linear regression lines, where higher S values correspond to a stronger dependence of complex stability on ionic strength. To evaluate the thermodynamic contribution of the salt effect, the standard Gibbs free energy changes were calculated for the complexation process at 298.15 K, both in the absence and presence of KCl, using eqn (5), as follows:

$$\Delta G^0 = -RT\ln(K). \quad (5)$$

The difference in ΔG^0 values (Table 6) between 2.9 and 3.5 kJ mol^{-1} reflects the stabilizing effect of KCl on the host–guest interaction. This moderate decrease in Gibbs free energy suggests that the presence of KCl enhances the complexation, potentially by reducing solvation competition or increasing the hydrophobic driving force for inclusion.

The data demonstrate that ionic strength is an important factor influencing the thermodynamics of host–guest interactions involving polar or dipolar guest molecules. The observed linear dependence between the inclusion constant and KCl concentration supports the hypothesis that electrostatic effects and solvation dynamics play a key role in modulating complex stability.

Table 5 Influence of the electrolyte on each host–guest system quantified by the S value

Host–guest system	1c• β-CD	1t• β-CD	1c• γ-CD	1t• γ-CD
S [M^{-2}]	99	130	227	408

Table 6 Free energy change for each host–guest system

	β-CD		γ-CD	
	1c•	1t•	1c•	1t•
ΔG (kJ mol^{-1}) (0 M KCl)	−9.40	−9.60	−10.62	−12.29
ΔG (kJ mol^{-1}) (0.25 M KCl)	−10.18	−11.17	−12.26	−13.88
ΔG (kJ mol^{-1}) (0.5 M KCl)	−11.30	−11.89	−13.14	−14.60
ΔG (kJ mol^{-1}) (1 M KCl)	−12.25	−12.88	−14.15	−15.68

Cyclic voltammetry measurements

The formation of inclusion complexes strongly affects not only the specific characteristics of the substrate, such as chemical reactivity, solubility or spectral properties, but also its electrochemical behaviour. Currently, the idea that electrochemical methods represent a suitable tool for analysing the formation process of these complexes has become increasingly popular, and has been found that experimental data from cyclic voltammetry, polarography or conductometry can be successfully used for estimating the inclusion constants (K_i) of cyclodextrin complexes.[10–13] Furthermore, it appears that electrochemical methods are highly sensitive to the formation of inclusion complexes even at low concentrations, allow for rapid monitoring without extensive sample preparation, and are easy to operate compared to spectroscopic or chromatographic techniques.[18]

In the present work, an attempt was made to analyse experimental data from cyclic voltammetry in terms of the diffusion coefficient (D) and peak current (I_p) to gain further insight into the inclusion of two cyclic nitroxide radical isomers (1c$^\bullet$ and 1t$^\bullet$) within β- and γ-CD.

Cyclic voltammetry experiments were performed in a 0.5 M KCl solution, and the very similar shapes of the voltammograms for the 1c$^\bullet$ and 1t$^\bullet$ isomers, together with their almost identical peak potential values (Fig. 6), suggest that the anodic oxidation of both radicals involves the same electrochemically irreversible mechanism. The effect of the sweep rate variation on the voltammetric responses was also investigated, and the characteristic patterns recorded for 1t$^\bullet$ (see the inset in Fig. 6) illustrate the results. It is worthy of note that, even for irreversible processes, the results of these experiments can provide some information, at least qualitative, concerning the diffusion coefficients of the chemical species involved in the overall electrochemical process, since the slope of the variation of the peak current as a function of the square root of the sweep rate is directly related to $D_{1/2}$ according to the irreversible Randles–Sevcik equation, as follows:

$$I_P = 2.99 \times 10^5 n(\alpha n_a)^{1/2} A c D^{1/2} v^{1/2}, \quad (6)$$

where $D^{1/2}$ is the diffusion constant, α stands for the transfer coefficient, n_a represents the number of electrons in the rate-determining step and the other symbols have their usual meaning, as follows: surface area of electrode (A), concentration of the electroactive species (c), and total number of electrons transferred (n). Fig. 7 shows the effect of the sweep rate variation on the voltammetric responses recorded for 1c$^\bullet$ and 1t$^\bullet$ both in the absence and in the presence of β-CD and γ-CD.

In all cases, the linear regression statistical analysis of $I_p = f(v^{1/2})$ yielded correlation coefficients of $R^2 > 0.99$, with a zero intercept indicating diffusion-controlled behavior. As illustrated in the inset of Fig. 6, an increase in the sweep rate led to an anodic shift in the peak potential, consistent with the irreversibility of the electrochemical oxidation process. The results in Fig. 7 show that, in the presence of the cyclodextrins, the slopes of the linear plot of I_p *vs.* $v^{1/2}$ are, for both 1c$^\bullet$ and 1t$^\bullet$, lower than those observed in their absence, indicating that the addition of the cyclodextrins results in a decrease in the diffusion coefficient, most likely due to an inclusion process between the cyclodextrin cavity and the guests. Also, it appears that compared to β-CD, the presence of γ-CD induces a more

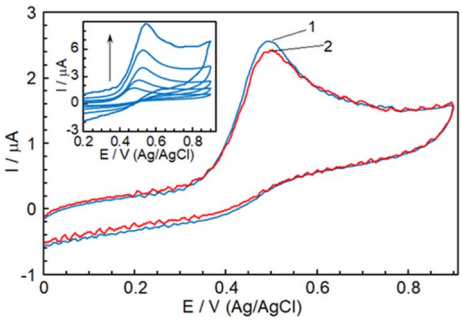

Fig. 6 Cyclic voltammograms (sweep rate = 20 mV s^{-1}) recorded for 1t$^\bullet$ (1) and 1c$^\bullet$ (2) (substrate concentration = 0.48 mM) in 0.5 M KCl. Inset: voltammetric responses for 1t$^\bullet$ recorded at 10, 20, 50, 100 and 200 mV s^{-1}. The arrow indicates the increasing sweep rate.

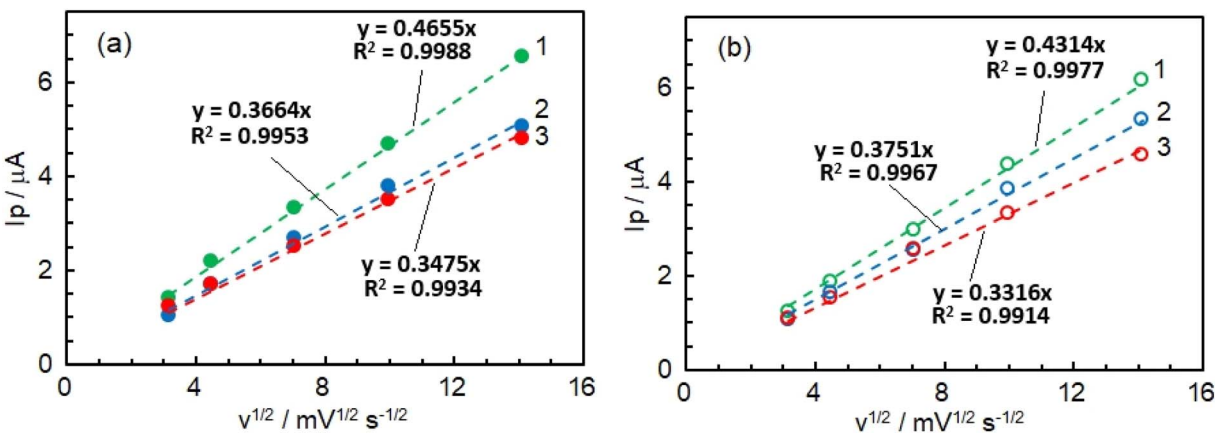

Fig. 7 Effect of the sweep rate variation on the anodic peak currents of 1t$^\bullet$ (a) and 1c$^\bullet$ (b) recorded in 0.5 M KCl in the absence of CD (1) and in the presence of 7.6 mM concentration of β-CD (2) and γ-CD (3). Substrate concentration = 0.48 mM.

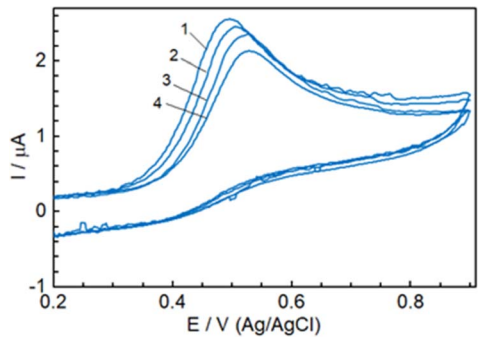

Fig. 8 Cyclic voltammograms (sweep rate = 20 mV s^{-1}) recorded for 1t• (0.48 mM) in 0.5 M KCl β-CD concentrations of 0 mM (1), 0.45 mM (2), 0.95 mM (3) and 7.6 mM (4).

significant decrease, as indicated by the corresponding decrease in the slopes in Fig. 7.

To estimate the K_i values of the inclusion complexes, the effect of an increase in β-CD and γ-CD concentration on the voltammetric response of the nitroxide radicals was investigated and the results are illustrated by the characteristic curves obtained for the 1t• β-CD system (Fig. 8).

It was observed that an increase in the cyclodextrin concentration led to a decrease in the peak current and a gradual anodic shift in the peak potential. These effects can be attributed to the decrease in the diffusion coefficient and to the fact that the inclusion process could hinder, to a certain extent, the adsorption of the electroactive species on the electrode surface, leading to an increase in the oxidation potential.

The inclusion constant, K_i, was calculated using the dissociation constant of the inclusion complex ($K_D = 1/K_i$), while K_D was estimated by means of the "electrochemical current method", using the following equation:[10]

$$I_p^2 = \frac{K_D}{[CD]_0}\left(I_{p,S}^2 - I_p^2\right) + I_{p,CD,S}^2, \quad (7)$$

where $I_{p,S}$ is the peak current recorded for either 1c• or 1t• in the absence of cyclodextrin, I_p is the peak current of 1c• or 1t• at various cyclodextrin concentrations, and $I_{p,CD,S}$ stands for the peak current corresponding to the guests included by cyclodextrin.

Table 7 Inclusion constants and free energy changes estimated using the electrochemical method

Host–guest system	K_i (M^{-1} dm^3)	ΔG (kJ mol^{-1})
1c• β-CD	408	−14.90
1t• β-CD	529	−15.55
1c• γ-CD	1396	−17.95
1t• γ-CD	2340	−19.23

Accordingly, the plot of I_p2 *vs.* $(I_{p,S}2 - I_p2)/[CD]_0$ should be a straight line with slope K_D, and the results obtained for 1c• and 1t• in the presence of β-CD and γ-CD are shown in Fig. 9.

Based on the estimated values of the inclusion constants, the free energy changes for the inclusion complexes (which express their stability) were also calculated, and the results are summarized in Table 7, together with the corresponding inclusion constants.

Apparently, in all cases, the inclusion constants estimated by the electrochemical current method are higher than those given by the EPR findings, in line with multiple published examples showing that cyclic voltammetry generally reports larger redox-state-dependent association constants than techniques that probe the neutral or radical species directly (*e.g.*, EPR, NMR, and ITC).[10,26–29] It is widely accepted that there are several reasons that can lead to such behaviour. Firstly, cyclic voltammetry measures the apparent binding strength of the oxidized (or reduced) guest, not necessarily the native state, and the inclusion host often binds such oxidized or reduced forms of the guest more strongly than the neutral form studied in EPR. This is because the electrochemically modified form may be more polar, charged or better fit geometrically and the redox conversion can strongly change hydrophobicity, charge distribution or dipole moment, making the inclusion more favourable.

Second, cyclic voltammetry can artificially enhance the strength of binding by changing the electron density of the

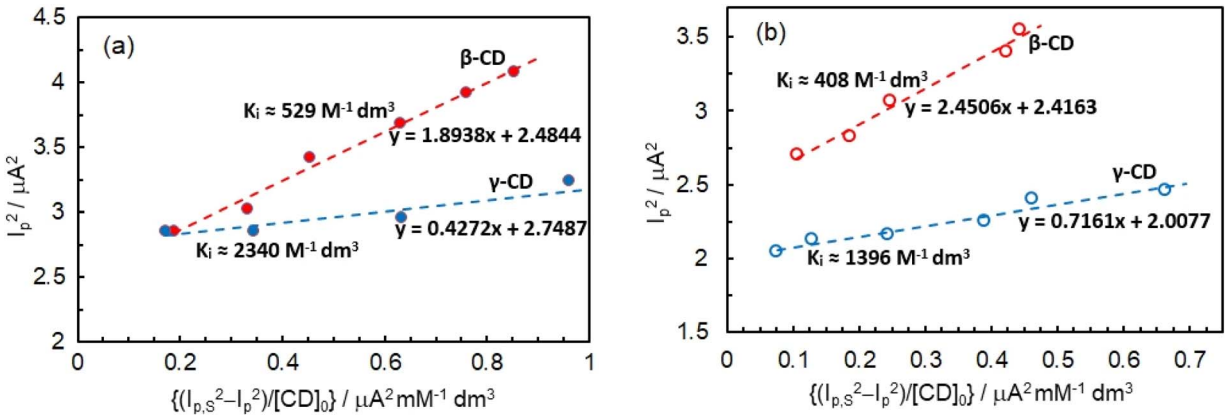

Fig. 9 Determination of K_i for the 1t•-CD (a) and 1c•-CD (b) complexes in 0.5 M KCl, using the electrochemical method.

guest, which can create a high binding affinity that applies only under electrochemical conditions, not in bulk solution. By contrast, EPR is less perturbative and reflects normal solution behaviour. Thirdly, cyclic voltammetry operates on a seconds time scale, where fast kinetic pre-association can appear as strong binding, while EPR measures equilibrium on longer time scales, more reflective of slow exchange or partial binding. Therefore, cyclic voltammetry sometimes exaggerates binding that is kinetically enhanced but not thermodynamically strong. Fourthly, the decrease in the voltammetric current might also be the result of a decline in the diffusion coefficient induced by a high guest content.

Nevertheless, the data in Table 7 also show, in agreement with the EPR findings, that the ΔG values of the guests included into the γ-CD cavity are always lower than those observed with β-CD, indicating the greater sensitivity of the guest–host interactions to the molecular size. Since the ΔG values express the stability of the inclusion complexes, it appears that γ-CD forms more stable complexes, probably due to the higher contact area between the guest molecule and the internal wall of the cyclodextrin.

Conclusions

The stereochemical differences between the nitroxide isomers significantly affect their complexation with cyclodextrins, with 1t$^{\bullet}$ displaying stronger binding and larger conformational changes due to the absence of OH···O═P intramolecular hydrogen bonding. γ-Cyclodextrin consistently forms more stable complexes than β-CD, particularly with 1t$^{\bullet}$. Increasing the electrolyte concentration enhances the complex stability by weakening solvation and electrostatic barriers, resulting in higher inclusion constants and more favourable thermodynamics. Electrochemical analyses support these findings, showing decreased diffusion coefficients and shifts in oxidation potential upon complex formation. These results underscore the key roles of molecular configuration and ionic environment in governing the stability and behaviour of host–guest complexes. Although the two physicochemical methods, EPR spectroscopy and cyclic voltammetry, do not provide similar values for the association constants corresponding to each radical/CD pair, the order of their variation is maintained.

Author contributions

Conceptualization and methodology: G. I. and S. R. A. M.; investigation: A. G. B., L. P., J.-P. J., M. T., T. S., and F. S.; formal analysis: G. I., A. G. B., N. S. and G. A.; writing-original draft preparation: all authors; writing-review and editing: A. G. B., S. R. A. M. and G. I.; and project administration and funding acquisition: G. I. and S. R. A. M. All authors gave approval to the final version of the manuscript.

Conflicts of interest

There are no conflicts to declare.

Data availability

The data supporting this article have been included within the article and as part of the supplementary information (SI). Supplementary information is available. See DOI: https://doi.org/10.1039/d6ra00820h.

Acknowledgements

We gratefully acknowledge the financial support from the project PNRR-III-C9-2023-I8 "Chemical host–guest molecular systems for health applications (OMRI for identification of inflammatory pathologies)", contract no. 760283/27.03.2024, the Ministry of Research, Innovation and Digitalisation, Romania, funded by the European Union–NextGenerationEU.

References

1 M. Lucarini and E. Mezzina, in *Electron Paramagnetic Resonance*, ed. B. C. Gilbert, D. M. Murphy and V. Chechik, Royal Society of Chemistry, Cambridge, 2011, vol. 22, pp. 41–70, DOI: 10.1039/9781849730877-00041.
2 E. G. Bagryanskaya and S. R. A. Marque, in *Electron Paramagnetic Resonance*, ed. V. Chechik and D. M. Murphy, Royal Society of Chemistry, 2017, vol. 25, pp. 180–235, DOI: 10.1039/9781782629436.
3 A. V. F. Neculae, G. Audran, S. Bourdillon, G. Ionita, J.-P. Joly, S. R. A. Marque, I. Matei and S. Mocanu, *J. Mol. Liq.*, 2022, **364**, 119983.
4 A.-G. Bucur, J.-P. Joly, I. Matei, S. R. A. Marque and G. Ionita, *Rev. Roum. Chim.*, 2025, **70**, 523–530, DOI: 10.33224/rrch.2025.70.7-8.16.
5 G. Ionita, S. Mocanu and I. Matei, *Phys. Chem. Chem. Phys.*, 2020, **22**, 12154–12165.
6 G. Ionita, A. Caragheorgheopol, H. Caldararu, L. Jones and V. Chechik, *Org. Biomol. Chem.*, 2009, **7**, 598–602.
7 K. Nagaraj, S. Kamalesu, S. Sakthinathan, T.-W. Chiu, S. Lokhandwala, N. M. Parekh and C. Karuppiah, *Spectrochim. Acta, Part A*, 2023, **286**, 122015, DOI: 10.1016/j.saa.2022.122015.
8 J. Mirković, J. Lović, M. Avramov-Ivić and D. Mijin, *Electrochim. Acta*, 2014, **137**, 705–713, DOI: 10.1016/j.electacta.2014.06.048.
9 O. Buriez, J. M. Heldt, E. Labbé, A. Vessières, G. Jaouen and C. Amatore, *Chem.–Eur. J.*, 2008, **14**, 8195–8203, DOI: 10.1002/chem.200800507.
10 M. Vilar and M. Navarro, *Electrochim. Acta*, 2010, **56**, 305–313, DOI: 10.1016/j.electacta.2010.08.079.
11 A. M. Martre, G. Mousset and P. Pouillen, *Electrochim. Acta*, 1988, **33**, 1465–1473, DOI: 10.1016/0013-4686(88)80141-5.
12 E. Junquera and E. Aicart, *Int. J. Pharm.*, 1999, **176**, 169–178, DOI: 10.1016/S0378-5173(98)00313-5.
13 K. Lozano, F. da Rocha Ferreira, E. G. da Silva, R. C. dos Santos, M. O. F. Goulart, S. T. Souza, E. J. S. Fonseca, C. Yanez, P. Sierra-Rosales and F. C. de Abreu, *J. Solid State Electrochem.*, 2018, **22**, 1483–1493, DOI: 10.1007/s10008-017-3805-y.

14 G. Audran, L. Bosco, P. Brémond, T. Butscher, J.-M. Franconi, K. Kabitaev, S. R. A. Marque, P. Mellet, E. Parzy, M. Santelli, E. Thiaudière and S. Viel, *RSC Adv.*, 2016, **6**, 5653–5670, DOI: 10.1039/C5RA23521A.
15 D. R. Duling, *PEST Winsim, Version 0.96*, National Institute of Environmental Health Sciences, Research Triangle Park, NC, 1996.
16 S. Stoll and A. Schweiger, *J. Magn. Reson.*, 2006, **178**, 42–55, DOI: 10.1016/j.jmr.2005.08.013.
17 M. J. Frisch, G. W. Trucks, H. B. Schlegel, G. E. Scuseria, M. A. Robb, J. R. Cheeseman, G. Scalmani, V. Barone, B. Mennucci, G. A. Petersson, H. Nakatsuji, M. Caricato, X. Li, H. P. Hratchian, A. F. Izmaylov, J. Bloino, G. Zheng, J. L. Sonnenberg, M. Hada, M. Ehara, K. Toyota, R. Fukuda, J. Hasegawa, M. Ishida, T. Nakajima, Y. Honda, O. Kitao, H. Nakai, T. Vreven, J. A. Montgomery Jr, J. E. Peralta, F. Ogliaro, M. Bearpark, J. J. Heyd, E. Brothers, K. N. Kudin, V. N. Staroverov, R. Kobayashi, J. Normand, K. Raghavachari, A. Rendell, J. C. Burant, S. S. Iyengar, J. Tomasi, M. Cossi, N. Rega, J. M. Millam, M. Klene, J. E. Knox, J. B. Cross, V. Bakken, C. Adamo, J. Jaramillo, R. Gomperts, R. E. Stratmann, O. Yazyev, A. J. Austin, R. Cammi, C. Pomelli, J. W. Ochterski, R. L. Martin, K. Morokuma, V. G. Zakrzewski, G. A. Voth, P. Salvador, J. J. Dannenberg, S. Dapprich, A. D. Daniels, Ö. Farkas, J. B. Foresman, J. V. Ortiz, J. Cioslowski and D. J. Fox, *Gaussian 09*, Gaussian, Inc., Wallingford, CT, 2009.
18 V. Chechik and G. Ionita, *Org. Biomol. Chem.*, 2006, **4**, 3505–3510, DOI: 10.1039/B607676A.
19 S. Mocanu, I. Matei, A. Leonties, V. Tecuceanu, A. Hanganu, Z. Minea, A. Stancu, E. I. Popescu and G. Ionita, *New J. Chem.*, 2019, **43**, 11233–11240, DOI: 10.1039/C9NJ01554J.
20 G. Audran, L. Bosco, P. Brémond, T. Butscher and S. R. A. Marque, *Appl. Magn. Reson.*, 2015, **46**, 1333–1342.
21 S. Acerbis, D. Bertin, B. Boutevin, D. Gigmes, P. Lacroix-Desmazes, C. Le Mercier, J.-F. Lutz, S. R. A. Marque, D. Siri and P. Tordo, *Helv. Chim. Acta*, 2006, **89**, 2119–2132, DOI: 10.1002/hlca.200690201.
22 A. Heredia, G. Requena and F. García Sánchez, *J. Chem. Soc., Chem. Commun.*, 1985, 1814–1815.
23 G. Audran, L. Bosco, P. Brémond, T. Butscher, S. R. A. Marque and S. Viel, *ChemPhysChem*, 2016, **17**, 3954–3963, DOI: 10.1002/cphc.201600647.
24 G. Audran, L. Bosco, P. Brémond, T. Butscher and S. R. A. Marque, *Org. Biomol. Chem.*, 2016, **14**, 1288–1292, DOI: 10.1039/C5OB02316E.
25 M. Okazaki and K. Kuwata, *J. Phys. Chem.*, 1984, **88**, 4181–4184, DOI: 10.1021/j150662a066.
26 Y. Ge, L. Miller, T. Ouimet and D. K. Smith, *J. Org. Chem.*, 2000, **65**, 8831–8838.
27 Y. M. Zhang, Y. Chen, R. J. Zhuang and Y. Liu, *Supramol. Chem.*, 2011, **23**, 372–378.
28 J. Liu, H. Lambert, Y. W. Zhang and T. C. Lee, *Anal. Chem.*, 2021, **93**, 4223–4230.
29 S. Yao, C. Falaise, S. Khlifi, N. Leclerc, M. Haouas, D. Landy and E. Cadot, *Inorg. Chem.*, 2021, **60**, 7433–7441.